WIND TUNNEL EVALUATION OF YF-12 INLET RESPONSE TO INTERNAL AIRFLOW DISTURBANCES WITH AND WITHOUT CONTROL

Gary L. Cole, George H. Neiner, and Miles O. Dustin
Lewis Research Center

SUMMARY

Experimental responses of the inlet's terminal shock and subsonic duct static pressures to internal airflow disturbances were obtained. The disturbances were produced by the aft bypass or a specially designed disturbance generator located at the diffuser exit. Transient and frequency responses were obtained from square wave and sinusoidal wave disturbances respectively. The main objective of this program was to determine the inlet responses with the inlet's duct-pressure-ratio control system active and to investigate ways of improving those responses within the limitations of the flight actuation hardware. Frequency response data were obtained first with inlet controls inactive. This indicated the general nature of the inherent inlet dynamics, assisted in the design of controls, and provided a baseline reference for responses with active controls. In addition, the data helped to validate a NASA-Lewis small-perturbation analysis of inlet dynamics.

All the control laws were implemented by means of a digital computer that could be programmed to behave like the flight inlet's existing analog control. The experimental controls were designed using an analytical optimization technique. The capabilities of the controls were limited primarily by the actuation hardware. The experimental controls provided somewhat better attenuation of terminal shock excursions than did the YF-12 inlet control. Controls using both the forward and aft bypass systems also provided somewhat better attenuation than those using just the forward bypass. However, the main advantage of using both bypasses is in the greater control flexibility that is achieved, allowing the inlet to have a more efficient (i.e., lower drag) operating point.

INTRODUCTION

An efficient propulsion system will be a key factor in the development of an economically viable commercial supersonic cruise aircraft. Propulsion studies (ref. 1) for the NASA supersonic cruise aircraft research (SCAR) program have identified new variable cycle engine concepts that offer potential performance gains over current engines. Studies also indicate that mixed-compression inlets will be used for cruise Mach numbers of about 2.2 and above. Such inlets offer lower cowl drag and higher total pressure recovery than do all external compression inlets. However, mixed-compression inlets are subject to an undesirable phenomenon known as unstart, which would be unacceptable on a

commercial transport. Unfortunately, the chances of a disturbance induced unstart increase as the inlet operates closer to its peak performance. Thus, a challenging problem is to design a control system that will allow the inlet to operate near its peak performance without unstart.

In general, control system design requires a dynamic model (measured experimentally or determined analytically) of the plant to be controlled. In the case of an inlet, it is necessary to know the response of duct pressures and terminal shock position to engine and atmospheric induced disturbances. Numerous experimental programs (e.g., refs. 2 to 14) have been conducted by NASA and industry to obtain inlet dynamics and control information for both real and simulated engine disturbances. Except for the program described in reference 14, the inlets were generally small scale and controls were implemented using analog computers.

Considerably less information is available relating to effects of atmospheric-type disturbances on mixed-compression inlets. Simulation of atmospheric disturbances in supersonic wind tunnels is extremely difficult, but some data have been obtained by oscillating flat plates and wedge shaped airfoils upstream of inlets (refs. 4 and 8). A recent analytical study (ref. 15) indicates that control of inlet terminal shock position against atmospheric disturbances may be of more concern than control against engine disturbances.

As part of the NASA program to investigate scale and flight effects on the steady-state and dynamic performance of the YF-12 aircraft inlet, a flight inlet from a YF-12 aircraft was tested in the Lewis 10- by 10-Foot Supersonic Wind Tunnel. The fact that the inlet was a flight article allowed the test to be unique. It was the first time that the dynamic response characteristics of a flight hardware mixed-compression inlet to simulated engine disturbances were evaluated in a wind tunnel (ref. 16). It provided an opportunity to systematically evaluate the bill-of-material inlet control system, including the control laws and actuation hardware (ref. 17). For convenience the inlet control laws were programed on the digital system described in reference 18 rather than in an analog mode like the actual aircraft system. With the trend being toward the use of digital computers for control, this also provided an opportunity to gain experience in the digital implementation of an actual flight control system. The success of this program provided some impetus and justification for the cooperative control program, planned for the YF-12 airplane (ref. 19). In addition, the YF-12 inlet program provided a timely application for a controller design method that uses the parameter optimization technique described in reference 20. Results using experimental shock position controllers and comparisons to results using the bill-of-material control are given in reference 21.

This paper summarizes the wind tunnel aspects of the YF-12 inlet dynamics and control program as detailed in references 16, 17, and 21. Experimental data, selected from those references, are presented showing the inlet normal shock and subsonic duct static-pressure responses to simulated engine disturbances, with and without control. For data shown in this paper the inlet angles of attack and sideslip were zero degrees and the Mach number was either 2.956 or 2.474.

SYMBOLS

Values are given in SI units. The measurements and calculations were made in U.S. customary units.

DPR	duct-pressure ratio (P_sD8/P_pLM)
E	error signal between a set-point commanded signal and the corresponding feedback signal, V
F	cost function
H	transfer function of feedback element $H = \left[\frac{\left(K_c \frac{s}{\omega_c} + 1\right)}{s}\right]$
K_c	gain of shock-position controller
M_∞	Mach number measured at nose boom
NAR	normalized amplitude ratio, $\frac{\left(\frac{\lvert Output \rvert}{\lvert Input \rvert}\right)_{\text{at input frequency}}}{\left(\frac{\lvert Output \rvert}{\lvert Input \rvert}\right)_{\text{at lowest frequency shown, without control}}}$
$P_{p,A}$	throat total-pressure probe (see fig. 6)
P_pLM	external cowl pitot-pressure measurement for YF-12 aircraft inlet DPR control signal, N/cm^2
$P_{s,A}$, $P_{s,B}$, ..., $P_{s,J}$, $P_{s,L}$, $P_{s,Q}$	static-pressure taps (see fig. 6)
P_sD8	static-pressure measurement for YF-12 aircraft inlet DPR control signal, N/cm^2
Q_n	noise-penalty weighting factor used in controller-gain optimization program
s	Laplace variable, 1/sec
U	control bypass door area, cm^2

α_∞	angle of attack measured at nose boom, deg
β_∞	angle of sideslip measured at nose boom, deg
ω_c	controller corner frequency, rad/sec

Superscripts:

$\overline{(\ )}$	mean value of ( )
$\dot{}$	derivative with respect to time

Subscripts:

D	disturbance
V	random measurement noise

APPARATUS

Inlet Model

A flight inlet from a YF-12 aircraft was used for this investigation in the 10- by 10-Foot Supersonic Wind Tunnel at Lewis Research Center. It is the same inlet that was used in the steady-state inlet performance investigations reported in references 22 and 23. Figure 1 is a schematic of the inlet showing variable geometry features and locations of bleeds and bypasses. The inlet is an axisymmetric, mixed-compression type and is sized at the design Mach number of 3+ to supply a J58 afterburning turbojet engine. The spike translates for inlet restart capability and operation at off-design Mach numbers.

Bleed regions for boundary layer control and shock stability are located on both the spike and cowl. Spike boundary-layer bleed is accomplished by a slotted surface on the spike. Cowl-boundary-layer bleed is provided by a combination flush slot and ram scoop referred to as the shock trap.

The inlet has two bypass sytems. The forward bypass is used to position the terminal shock by means of a duct-pressure-ratio (DPR) control, to be described later. It is also used to bypass large amounts of airflow during an inlet restart cycle. The aft bypass provides air for some engine cooling and aids the forward bypass in matching the inlet airflow to the engine requirement at Mach numbers below 3.0. In flight, the aft-bypass is set by the pilot at one of three discrete positions. For the wind-tunnel tests, the discrete positioning mechanism was replaced with an electrohydraulic servomechanism to provide continuous position control like that of the forward bypass. Frequency responses of forward and aft bypass position to position commands are shown in figure 2. The amplitude ratio responses were normalized by dividing by the respective amplitude ratios at 0.1 hertz.

The inlet was attached to a boiler-plate nacelle and the complete assembly was strut-mounted in the wind tunnel (fig. 3). Inside the nacelle was a cold-

pipe assembly. An airflow-disturbance generator was strut-mounted in the cold pipe near the diffuser exit (fig. 3). The assembly, shown in more detail in figure 4, consisted of five sliding plate valves that were hinged so that they could expand like an umbrella. The amount of assembly expansion and the position of each sliding valve was remotely controlled by electrohydraulic servomechanisms. Airflow across the assembly was choked. Thus, actuation of the sliding plate valves provided a means of simulating perturbations in engine corrected airflow. The frequency response of sliding-valve position to position command is shown in figure 5. The amplitude response was normalized by dividing by the amplitude at 1 hertz. Note that its response has a much wider frequency range than that of the two bypass systems. Details of the sliding valve servosystem design are given in reference 24.

Inlet angle of attack could be remotely adjusted by means of the strut during a tunnel run. Inlet angle of sideslip could be adjusted only between runs. The angles of attack and sideslip were 0° for all data shown in this paper.

Additional details concerning the inlet systems and wind tunnel installation are given in reference 25. Reference 26 also gives additional information regarding the F-12 series aircraft propulsion system.

Instrumentation

The pressure instrumentation consisted of high-response strain-gage pressure transducers closely coupled to static taps and total probes located on the inlet internal-cowl surface. Relative locations of the pressure measuring stations are shown in figure 6. Exact axial locations are given in figure 11 of reference 16. The response of each transducer and its connecting line was flat within 0 to +0.5 decibel and had negligible phase shift in the frequency range of 0 to 100 hertz.

Duct static pressure, P_sD8, is a measurement of the pressure from eight manifolded static-pressure taps, shown in figure 6. A high-response pressure transducer of the type described previously also was used to measure the duct static pressure. The duct static pressure is of interest because it is one of two pressures used to determine duct pressure ratio DPR, the feedback signal for the YF-12 forward bypass control. The DPR system was implemented so that its response would be nearly identical to that of the flight YF-12 system. However the ratio was computed electronically rather than by the aircraft mechanical sensor.

The outputs of the pressure transducers connected to static-pressure taps $P_{s,A}$ to $P_{s,J}$ were used as inputs to an electronic terminal-shock-position sensor. The shock sensor was used to obtain a measure of the response of inlet terminal-shock position to airflow perturbations. The frequency response of terminal-shock position as measured by the sensor to actual shock position was found to be essentially flat with no more than 15° phase lag for frequencies in the range of 0 to 40 hertz. A detailed description of the sensor design and

performance is given in reference 27. Additional details regarding instrumentation are given in reference 25.

EXPERIMENTAL SETUP AND CONDITIONS

Figure 7 is a schematic of the wind-tunnel experimental setup. Shown are the inlet, the flow paths of the command signals to the servomechanisms, the flow paths of the measured inlet signals, and a general-purpose digital system. The digital system was used to program both the aircraft and experimental inlet terminal-shock-position controllers that will be described later. It also controlled the sequencing of the experiment and performed calculations to provide an immediate on-line display of results at the completion of each frequency response test. Some characteristics and capabilities of the digital computer system are given in table I and additional details of the overall system are provided in reference 18.

The inlet geometry configuration and terminal shock operating point were generally about the same as those that would be set by the YF-12 aircraft inlet-control system for corresponding flight conditions. Average free-stream wind tunnel conditions, at which data shown in this paper were taken, were as follows: Mach number, 2.956; total temperature, 373 K; Reynolds number per meter, 4.01×10^6 or Mach number, 2.474; total temperature, 310 K; Reynolds number per meter, 4.91×10^6. The Reynolds numbers correspond to values within the flight envelope of the aircraft.

RESULTS AND DISCUSSION

Responses without Inlet Control

Responses of several inlet variables to simulated engine airflow perturbations without inlet control were obtained first. This indicated the general nature of the inherent inlet dynamics, assisted in the design of controls and provided a baseline reference for responses with active controls. In addition, the data helped to validate a NASA-Lewis small-perturbation analysis of inlet dynamics.

Experimental responses of terminal shock position and three subsonic duct static pressures to the airflow disturbance generator, at the Mach 2.956 condition, are shown in figure 8. Responses based on the small-perturbation analysis of reference 28 are also shown for comparison. The equations governing terminal-shock position were derived by taking continuity, momentum, and energy balances across the shock and accounting for a moving shock. The subsonic duct is represented by sets of one-dimensional wave equations. In general, the amplitude experimental responses have an initial rolloff followed by one or more resonances. A particularly prominent peak occurs at about 40 hertz, except for P_sD8. The greater attenuation of P_sD8 is due to its measuring system line and volume dynamics. The phase data are generally dom-

inated by a delay time. This was demonstrated in reference 16 which showed phase angle to be linear with frequency above frequencies of 20 to 40 hertz, depending on signal location. The characteristics of the YF-12 inlet are similar to those of the inlets of references 8, 11, and 13. However, scale effects on the dynamics of the inlets cannot be determined explicitly because none of the inlets are the same geometrically. Also, overboard bypasses (holes in the side of the subsonic duct) were not similarly located and disturbances occurred at different locations which would modify the organ pipe frequency of the ducts. In general, the rolloff of the YF-12 inlet is more rapid than for the other inlets because of its greater subsonic-duct volume and it resonates at a lower frequency because of its greater subsonic-duct length. Although corresponding frequency response data were not available from flight for comparison, the results would be expected to be the same for a corresponding inlet operating point condition, except for a modification due to temperature. In flight, the stagnation temperature for the Mach 2.956 condition would be approximately 1.6 times the wind-tunnel value. Therefore, the duct delay and fill times would be shorter in flight than in the tunnel because the speed of sound is higher. The approximate inlet response expected for the flight condition can be determined by multiplying the tunnel disturbance frequencies by the square root of the ratio of flight temperature to tunnel temperature. For example, the resonant peak that occurs at 40 hertz in the tunnel should occur at approximately 51 hertz in flight.

Before discussing the comparison of the analytical and experimental responses in figure 8, a few observations will be made concerning the inlet analysis. Calculation of parameters used in the analysis can generally be determined analytically with satisfactory accuracy. One exception is an area parameter common to most inlet analyses. The parameter, A'/A, is defined as the ratio of the axial rate of change of duct area A' to the duct area A, evaluated at the shock operating point. The steady state gain of shock position to an airflow disturbance in the subsonic duct is a strong function of A'/A. It has been found that if the value of A'/A used in the analysis is based on inlet geometry the analytical value of the gain is always higher than the value measured experimentally. This is believed to be due to effects of shock/boundary-layer interaction that are unaccounted for and to inadequate modeling of the boundary layer bleed systems. By knowing the experimental value of the gain, an effective value of A'/A can be calculated so that the steady-state gains will match exactly. For the inlet of reference 8 the effective value of A'/A was found to range from 2 to 4 times the geometric value, depending on the boundary-layer bleed configuration. For the case of figure 8, the effective value was 2.5 times the geometric value.

A similar difficulty exists in matching the steady-state gains of static pressures in the subsonic portion of the duct to the airflow disturbance. In this case the analytically-determined value of the gain is lower if the analysis is based strictly on inlet geometric areas. The major parameter affecting this mismatch of gains is the duct Mach number at the pressure measuring station. The duct Mach number, of course, depends on the boundary layer. Experimental steady state data can also be used to make the gains match. This was not done in the case of figure 8. In general, the phase response data of

the terminal shock and the static pressures are not significantly affected by these parameters.

The agreement between the experimental and analytical responses shown in figure 8 is generally typical of that obtained with the smaller scale inlets of references 8 and 11. Agreement in phase angle is usually excellent. Amplitude ratio agreement, although not as good as phase in an absolute sense over the entire frequency range, is generally good in terms of the rolloff and resonant frequencies.

Reference 16 also presents amplitude ratio data showing how YF-12 inlet response varies with free-stream Mach number, angle of attack, shock operating point and amount of forward bypass opening. The most significant variations in initial rolloff and resonant frequency conditions were found at different free-stream Mach number conditions. The different results are attributed to combinations of changes in tunnel total temperature, spike position, forward and aft bypass opening, terminal shock operating point, and simulated-engine corrected airflow. The inlet also exhibited an extreme resonant condition with the inlet operating at a higher than normal value of duct pressure ratio, DPR. In that case the shock was near or in the shock trap, which acts in a nonlinear manner. Also, this test may have excited a resonance in the secondary airflow duct (behind the shock trap).

Frequency responses of inlet signals to both the forward and aft bypasses were also obtained. However, there is less confidence in those data because bypass motion did not remain sinusoidal above a frequency of about 1 hertz.

Responses With Inlet Control

YF-12 aircraft inlet control system. - A simplified diagram of the YF-12 aircraft inlet control system is shown for normal started-inlet conditions in figure 9. The system manipulates the spike and forward bypass positions. An air data computer converts pressures measured at the airplane nose boom to aircraft flight Mach number and angles of attack and sideslip. These flight parameters are then used as inputs to the control system. The spike is translated to provide the necessary contraction ratio at each Mach number. The purpose of the control that manipulates the forward bypass is to maintain the terminal shock at the desired location. Shock position is sensed indirectly by means of the duct-pressure-ratio, DPR. Both spike position and commanded value of DPR are scheduled as functions of Mach number and both are biased by angles of attack and sideslip and aircraft normal acceleration. In flight the schedules are implemented by means of cams, and associated filtering and compensation are accomplished electronically by analog equipment.

During the wind-tunnel program the inlet-control schedules and associated filtering and compensation were implemented on the general purpose digital system (fig. 7). This will also be done in the cooperative control program of reference 19. Since an isolated inlet was tested, the airplane air data computer and normal acceleration terms were unavailable. Therefore, the digital system was also used to calculate the airplane flight conditions that would

correspond to the measured local inlet conditions. The calculations were based on data obtained from the YF-12 flight program and from wind tunnel tests of a YF-12 scale model. The acceleration term was omitted.

The digital computer program was performed on a priority-interrupt basis at seven levels. About 25 percent of the time was spent checking the priority-interrupt structure to determine what should be calculated next and where its data should come from. About 50 percent of the time was spent calculating the spike and DPR setpoints (commanded values) and the forward bypass control. The remaining 25 percent of the time was spent on auxiliary routines, such as frequency response calculations. Updates of the setpoint values and the forward bypass control occurred every 9 milliseconds and 2 milliseconds, respectively. The control update time was faster than necessary, since the forward bypass can't respond to commands much beyond 1 hertz. According to sampled-data theory, the setpoint update time of 9 milliseconds would allow recognition of signals with frequency content of about 50 hertz or less. This was more than adequate for the wind tunnel tests, since conditions were constant. However, in flight, rapid variation of atmospheric conditions (e.g., ambient temperature and pressure and relative velocity due to gusts) can cause an undesirable response of the inlet's terminal shock (ref. 15). Hence, a more rapid update rate of the setpoint values to the control might be required. One consequence of inadequate sampling is that the bypass system will drive the inlet shock at a frequency that is different from the disturbance frequency (ref. 29). Controller dynamics were programmed using the advanced Z-transform representation of the transfer-function.

Closed-loop amplitude responses of P_sD8 and the output of the terminal-shock-position sensor to the airflow disturbance generator at Mach 2.474 conditions are compared to the open loop responses in figure 10. (The response of DPR would be the same as that for P_sD8, since P_pLM was constant.) The closed-loop responses show that the control system is able to attenuate disturbance induced shock motions, relative to the open-loop, for disturbances frequencies only below 1 to 1.5 hertz. The control is limited primarily by the speed of response of the forward bypass system. In the frequency range of 1.5 to 10 hertz the P_sD8 response shows considerable amplification relative to the open-loop, with a peak amplitude ratio of about 2.5 at 2 hertz. This indicates that the control is reinforcing the disturbance. The extent of the peaking can be reduced by decreasing the controller gain, but then the attenuation at the low frequencies (0.2 Hz) would not be as great. Also the speed of response would be slower. The closed-loop response eventually rejoins the open-loop response, indicating that the control system has become ineffective. Closed-loop frequency responses were also obtained at higher Mach numbers (ref. 17). The response at Mach 2.956 (ref. 17) showed very little peaking above the open-loop response. Therefore, for the operating conditions in the wind tunnel, the inlet closed-loop response was more stable at Mach 2.956 than at Mach 2.474.

Open and closed-loop transient responses to a step change in the airflow disturbance generator are shown in figure 11 for the same operating condition as that for the frequency response of figure 10. The uncontrolled change in shock position (fig. 11(a)) is approximately 13.7 centimeters. The noise-free

portion of the shock sensor trace occurs when the shock has moved upstream of pressure tap $P_{s,A}$ (fig. 6). The shape of the response of pressure $P_{s,I}$ is very similar to the shock response. The closed-loop transient (fig. 11(b)) shows that the control system responds rather unstably to the disturbance. The forward bypass oscillates at about 2 hertz with no evidence that the oscillation will die out. The frequency of the oscillation corresponds to the frequency at which peaking occurs (fig. 10). After the disturbance occurs, the control system drives the shock through some peak-to-peak excursions that are actually greater (about 16 cm) than without control. This response is undesirable and indicates a need for a controller gain adjustment at the Mach 2.474 condition.

Figure 12 shows the transient response at the Mach 2.474 condition with the loop gain reduced to about one-third of its value for the transient of figure 11. The forward bypass still exhibits an overshoot followed by some ringing which tends to die out, but the oscillations are not nearly as severe as for the case of figure 11. The forward bypass is seen to open more rapidly than it closes - an observation not quite so apparent in figure 11. The system was designed that way to allow the inlet to move quickly away from an unstart condition.

Transient responses were also obtained for the Mach 2.956 condition and are shown in reference 17. The closed-loop transient response was similar to that for the reduced gain case at Mach 2.474, indicating a better choice of gain for the Mach 2.956 condition. However, the transient response was more oscillatory than would have been expected from the closed-loop frequency response. This may be due, in part, to nonlinearities in the system.

The frequency response and transient data just discussed indicate that both types of testing are valuable. As will be discussed later, the open-loop frequency response data can be used for designing controllers. However, the closed-loop frequency response may not indicate potential problems that are revealed by transient tests. In simulating the control system, the actuation hardware should be accurately simulated including nonlinearities like hysteresis and friction. Or better yet, actual flight hardware should be used. Care must be taken to be sure that closed-loop responses are sufficiently stable at all conditions.

The closed-loop transient response of the inlet to an aft-bypass disturbance is shown in figure 13. The response is seen to be basically the same as that of figure 12. However, this transient revealed an oscillation of the aft bypass system that did not occur during transients when the DPR control system was inactive. A similar action occurred at the Mach 2.956 condition (ref. 17). This indicates that a coupling, although small, does exist between the aft-bypass servosystem and the DPR control system. The origin of the coupling is unknown, but could be due to either an aerodynamic flow force or a structural vibration. It should be kept in mind that the aft-bypass actuator used in the wind tunnel tests is not the same as the standard one used on the aircraft. However, as will be discussed later, it may be beneficial to use both overboard bypass and secondary bypass servo-driven systems for inlet control. Hence, the potential for interaction exists that may only be revealed by experimental tests.

Experimental inlet control systems. - An investigation was conducted to determine if control of the YF-12 inlet terminal shock could be improved by improving the controller dynamics and/or by using the aft bypass system or engine speed (simulated) to augment the forward bypass system (ref. 21). These tests were all conducted at the Mach 2.956 condition.

Figure 14 shows block diagrams of the four types of experimental controls that were tested. The type I system is like the aircraft inlet system except that it uses a different feedback signal and controller. Types I and II used either $P_{s,I}$ or the shock-position sensor output as the feedback signal. The closed-loop responses using either variable were not significantly different, so, unless noted otherwise, only results with $P_{s,I}$ feedback will be shown. Types III and IV controls used $P_{s,I}$ as the feedback signal. For types III and IV, a second loop causes reset action of the forward bypass by means of either the aft-bypass or the sliding-valves of the airflow-disturbance generator. The action of the sliding valves was slowed down to simulate realistic changes in engine speed. The controller for all four types was a proportional-plus-integral filter function having the general form

$$H = \frac{K_c\left(\frac{s}{\omega_c} + 1\right)}{s}$$

Optimal fixed-form controller parameters (K_c and ω_c) were determined by using a computerized frequency-domain technique described in reference 20 as opposed to an optimal time-domain technique (e.g., ref. 30). The technique is based on minimization of a cost function which included the system regulation error (E_D) due to the disturbance and the control power ($\overline{\dot{U}_V^2}$) due to measurement noise. The cost function can be stated in equation form as

$$F = \overline{E_D^2} + Q_n\overline{\dot{U}_V^2}$$

where Q_n is a noise-penalty weighting factor. The computer technique requires as input the transfer function for the uncontrolled inlet dynamics and actuation hardware dynamics. The computer then calculates the expected closed-loop frequency response and the cost function while searching for the optimum gains. The optimum controller gains, determined for various values of Q_n, were evaluated experimentally to find the most acceptable values of K_c and ω_c. This method provided a simpler and quicker means of arriving at controller parameters than do the classical methods such as the root locus approach that was used in reference 9. This would be especially true if more than two controller parameters were involved. The optimization approach would be even more useful in a case like the experimental program of reference 12 where the inlet had a high response (100 Hz) overboard bypass system and the control feedback signals were very noisy due to an inlet instability.

A comparison of computed analytical and experimentally measured closed-loop frequency responses for type-I controls are shown in figure 15. Results are presented for a range of values of the noise-penalty weighting factor Q_n. All of the results exhibit similar characteristics. The increase in amplitude

ratio with frequency below 1 hertz is expected because of the integral control action. As Q_n decreases the noise penalty decreases and there is a corresponding increase in controller gain. Therefore the control loop-gain increases, accounting for the greater attenuation at disturbance frequencies of about 1.5 hertz and below. The agreement between analytical and experimental results is quite good except in the vicinity of 2 hertz, when Q_n was 0.01. The same kind of discrepancy has been observed before when control system loop gains were high (e.g., ref. 9). This phenomenon was investigated more thoroughly in another test as shown in figure 16. In this case data were taken at closer frequency intervals in the vicinity of a peak like the one that occurred in figure 15. As for the results of figure 15, the sudden increase in amplitude ratio occurred only when Q_n was 0.01. The sudden change in the frequency response is characteristic of a jump resonance and indicates that the loop gain finally became large enough so that nonlinearities in the system had a significant effect on the closed-loop response. The inlet response is certainly not linear for large excursions of the terminal shock. A linearized inlet model will predict higher allowable gains than can be achieved in the real system. Thus, care must be exercised in interpreting control results from a linearized inlet model, or alternately the system nonlinearities must be accurately simulated.

Generally, it was found that a noise-penalty weighting factor, Q_n, of 0.1 resulted in good performance for the type I and II controllers. The closed-loop frequency responses generally showed good attenuation of disturbance induced shock motion at the low end of the frequency scale. At the same time, the jump resonance phenomenon of figures 15 and 16 was avoided. These controllers were also tested with the reset action of the type III and IV controls. These types of control had been investigated earlier using an actual engine (refs. 31 and 32). Figure 17 shows a comparison of the closed-loop responses for the four types of experimental control systems along with the YF-12 aircraft inlet duct-pressure-ratio control. The results indicate that, although the experimental controls gave somewhat better performance (greater attenuation), the airplane control was pretty well optimized for the Mach 2.956 condition. The optimization procedure couldn't produce a control that was significantly better than the airplane control because the forward bypass actuation hardware was the major limiting factor. Note that the addition of the reset action had a stabilizing effect on the control as evidenced by the decrease in peaking at the resonant frequency for the type III and IV controls. Additional frequency response data are given in reference 21.

Transient responses were obtained for the type I, III, and IV controls (ref. 21). No significant differences between the type I and airplane controls were observed. Figure 18 shows a transient response that illustrates the reset action of the type III control system. Just after the disturbance occurs (point 1) the forward-bypass opens (point 2) to bring the shock back to its desired position (point 3). The aft-bypass is then slowly opened by the controller reset action (point 4), which allows the forward-bypass to go closed again (point 5) to a lower drag condition. The same sequence of events occurs (points 6, 7, 8, 9, and 10) when the disturbance-generator area opens. The different rates of reset are due to the fact that the aft-bypass actuator moves faster in the closing direction than in the opening direction. The action of

the type IV control system is similar except that the reset of the forward bypass was caused by a change in engine speed simulated by the airflow-disturbance generator. Neither the type III or type IV control systems offer a response that is much faster than the type I and II or airplane control systems. The advantage is in the greater control flexibility that is achieved, allowing the inlet to have a more efficient (i.e., lower drag) operating point. This would be especially desirable for a commercial supersonic cruise aircraft. Rapid reset of the forward bypass might also be used to minimize the effects of propulsion system interaction with the lateral and longitudinal directional-control characteristics that have been noted in references 33 and 34. It is hoped that this kind of control can be demonstrated during the cooperative control flight program of reference 19.

SUMMARY OF RESULTS

The response of terminal-shock position and static pressures in the subsonic duct of a YF-12 aircraft flight-hardware inlet to perturbations in simulated engine corrected airflow were obtained with and without inlet control. Both the YF-12 duct-pressure-ratio DPR control and experimental controls which had optimal, fixed-form terminal-shock-position controllers were used. In some cases the experimental controls reset the forward bypass to the desired position by trading either aft-bypass area or a change in simulated engine speed for forward-bypass area.

The open-loop frequency-response amplitude ratio data generally exhibited a rolloff characteristic followed by one or more resonances. The results were similar to those obtained for small scale inlets except that the rolloff and first resonance occurs at lower frequencies for the YF-12 inlet. This is due to the larger volume and greater length of the YF-12 inlet subsonic duct. Phase data were found to be dominated by a delay time at frequencies above 20 to 40 hertz depending on signal location. The responses in in-flight should be similar except for a shift in the frequency scale due to a difference in temperature. Closed-loop frequency responses, calculated from open-loop transfer functions of the individual components of the system, generally gave good agreement with experimentally measured results. However, when controller gains were too high, agreement was poor in the vicinity of a resonance because nonlinearities in the system had a large effect.

Frequency responses with the YF-12 DPR control system active showed attenuation of disturbance-induced shock excursions for frequencies of about 1 hertz and below. Above 1 hertz the control was either ineffective or made the shock excursion worse. Both frequency and transient response data indicated that the inlet closed-loop response was less stable at some Mach numbers than at others. In cases where the aft bypass was used to disturb the inlet, with the DPR control system active, an undesirable coupling of unexplained origin caused the aft-bypass servosystem to oscillate. Although the aft-bypass actuator used for these tests is not the same as the standard one used on the airplane, it is important to recognize that the potential for such a coupling does exist.

The experimental terminal-shock-position controls did not perform significantly better than the YF-12 DPR control. In general, the speed of response of the forward bypass is a major limiting factor for all of the controls. The controls that reset the forward bypass were found to operate more stably than the others. Another advantage of the controls with reset is the greater degree of control flexibility, allowing the inlet to operate at a more efficient (i.e., lower drag) operating point.

REFERENCES

1. Willis, E.; and Welliver, A. D.: Variable-Cycle Engines for Supersonic Cruise Aircraft. AIAA Paper 76-759, July 1976.

2. Chun, K. S.; and Burr, R. H.: A Control System Concept for an Axisymmetric Supersonic Inlet. J. Aircr., vol. 6, no. 4, July-Aug. 1969, pp. 306-311.

3. Schweikhardt, R. G.; and Grippe, R. P.: Investigations in the Design and Development of a Bypass Door Control System for an SST Axisymmetric Intake Operating in the External Compression Mode. AIAA Paper 70-695, June 1970.

4. Investigations of Supersonic Transport Engine Inlet Configurations. (LAC-603220, Lockheed Aircraft Corp.; NASA Contract NAS2-2363.) NASA CR-68399, 1965.

5. Inlet-Exhuast-Thrust Reverser Program for the Commercial Supersonic Transport. LAC-596884, Lockheed Aircraft Corp., Aug. 1964; ASD Contract No. AF33(657)-11419 for FAA. AD-367328L.

6. Martin, Arnold W.; Kostin, Leonard C.; and Millstone, Sidney D.: Dynamic Distortion at the Exit of a Subsonic Diffuser of a Mixed Compression Inlet. NASA CR-1644, 1970.

7. Martin, Arnold W.; Beaulieu, Warren D.; and Kostin, Leonard C.: Analysis and Correlation of Inlet Unsteady Flow Data. NA-71-1146, North American Rockwell Corp., 1971.

8. Wasserbauer, Joseph F.: Dynamic Response of a Mach 2.5 Axisymmetric Inlet with Engine or Cold Pipe and Utilizing 60 Percent Supersonic Internal Area Contraction. NASA TN D-5338, 1969.

9. Neiner, George H.; Crosby, Michael J.; and Cole, Gary L.: Experimental and Analytical Investigation of Fast Normal Shock Position Controls for a Mach 2.5 Mixed-Compression Inlet. NASA TN D-6382, 1971.

10. Cole, Gary L.; Neiner, George H.; and Crosby, Michael J.: An Automatic Restart Control System for an Axisymmetric Mixed-Compression Inlet. NASA TN D-5590, 1969.

11. Baumbick, Robert J.; Neiner, George H.; and Cole, Gary L.: Experimental Dynamic Response of a Two-Dimensional, Mach 2.7, Mixed-Compression Inlet. NASA TN D-6957, 1972.

12. Cole, Gary L.; Neiner, George H.; and Baumbick, Robert J.: Terminal Shock Position and Restart Control of a Mach 2.7, Two-Dimensional, Twin-Duct Mixed-Compression Inlet. NASA TM X-2818, 1973.

13. Baumbick, Robert J.; Wallhagen, Robert E.; Neiner, George H.; and Batterton, Peter G.: Dynamic Response of Mach 2.5 Axisymmetric Inlet with 40 Percent Supersonic Internal Area Contraction. NASA TM X-2833, 1973.

14. Batterton, P. G.; Arpasi, D. J.; and Baumbick, R. J.: Digital Integrated Control of a Mach 2.5 Mixed-Compression Inlet and an Augmented Mixed-Flow Turbofan Engine. NASA TM X-3075, 1974.

15. Cole, Gary L.: Atmospheric Effects on Inlets for Supersonic Cruise Aircraft. AIAA Paper 77-874, July 1977.

16. Cole, Gary L.; Cwynar, David S.; and Geyser, Lucille C.: Wind-Tunnel Evaluation of the Response of a YF-12 Aircraft Flight Inlet to Internal Airflow Perturbations by Frequency-Response Testing. NASA TM X-3141, 1974.

17. Neiner, George H.; Arpasi, Dale J.; and Dustin, Miles O.: Wind-Tunnel Evaluation of YF-12 Aircraft Inlet Control System by Frequency-Response and Transient Testing. NASA TM X-3142, 1975.

18. Arpasi, Dale J.; Zeller, John R.; and Batterton, Peter G.: A Genral Purpose Digital System for On-Line Control of Air-breathing Propulsion Systems. NASA TM X-2168, 1971.

19. Reukauf, Paul J.; Burcham, Frank W., Jr.; and Holzman, Jon K.: Status of a Digital Integrated Propulsion/Flight Control System for the YF-12 Airplane. AIAA paper 75-1180, Sep. 1975.

20. Seidel, Robert C.; and Lehtinen, Bruce: Control System Design Using Frequency Domain Models and Parameter Optimization, With Application to Supersonic Inlet Controls. NASA TM X-3108, 1974.

21. Neiner, George H.; Seidel, Robert C.; and Arpasi, Dale J.: Wind-Tunnel Evaluation of Experimental Controls on YF-12 Aircraft Flight Inlet by Frequency-Response and Transient Testing. NASA TM X-3143, 1975.

22. Cubbison, Robert W.: Wind-Tunnel Performance of an Isolated, Full-Scale, YF-12 Aircraft Inlet at Mach Numbers Above 2.1. NASA TM X-3139, 1978.

23. Cubbison, Robert W.: Effects of Angle of Attack and Flow Bypass on Wind-Tunnel Performance of an Isolated, Full-Scale, YF-12 Aircraft Inlet at Mach Numbers Above 2.075. NASA TM X-3140, 1978.

24. Webb, John A., Jr.; Mehmed, Oral; and Hiller, Kirby, W.: Improved Design of a High Response Slotted Plate Overboard Bypass Valve for Supersonic Inlets. NASA TM X-2812, 1973.

25. Wind-Tunnel Installation of Full-Scale Flight Inlet of YF-12 Aircraft for Steady-State and Dynamic Evaluation. NASA TM X-3138, 1974.

26. Campbell, David H.: F-12 Series Aircraft Propulsion System Performance and Development. J. Aircr., vol. 11, no. 11, Nov. 1974, pp. 670-676.

27. Dustin, Miles O.; Cole, Gary L.; and Neiner, George H.: Continuous-Output Terminal-Shock-Position Sensor for Mixed-Compression Inlets Evaluated in Wind Tunnel Tests of YF-12 Aircraft Inlet. NASA TM X-3144, 1974.

28. Willoh, Ross G.: A Mathematical Analysis of Supersonic Inlet Dynamics. NASA TN D-4969, 1968.

29. Neiner, George H.; Cole, Gary L.; and Arpasi, Dale J.: Digital-Computer Normal Shock Position and Restart Control of a Mach 2.5 Axisymmetrix Mixed-Compression Inlet. NASA TN D-6880, 1972.

30. Zeller, John R.; et al.: Analytical and Experimental Performance of Optimal Controller Designs for a Supersonic Inlet. NASA TN D-7188, 1973.

31. Cole, Gary L.; Neiner, George H.; and Wallhagen, Robert E.: Coupled Supersonic Inlet-Engine Control Using Overboard Bypass Doors and Engine Speed to Control Normal Shock Position. NASA TN D-6019, 1970.

32. Paulovich, Francis J.; Neiner, George H.; and Hagedorn, Ralph E.: A Supersonic Inlet-Engine Control Using Engine Speed as a Primary Variable for Controlling Normal Shock Position. NASA TN D-6021, 1971.

33. Gilyard, Glenn B.; Berry, Donald T.; and Belte, Daumantes: Analysis of a Lateral-Directioanl Airframe/Propulsion System Interaction of a Mach 3 Cruise Aircraft. AIAA Paper 72-961, Sep. 1972.

34. Powers, Bruce G.: Phugoid Characteristics of a YF-12 Airplane with Variable-Geometry Inlets Obtained in Flight Tests at a Mach Number of 2.9. NASA TP-1107, 1977.

TABLE I. - DIGITAL SYSTEM CAPABILITIES

Digital computer	
Magnetic core memory size, words	16 384
Word length, bits plus parity	16
Memory cycle time, nsec	750
Add time, μsec	1.5
Multiply time, μsec	4.5
Divide time, μsec	8.25
Load time, μsec	1.5
Indirect addressing	Infinite
Indexing	Total memory
Priority interrupts	28 separate levels
Index registers	2
Interval timers	2

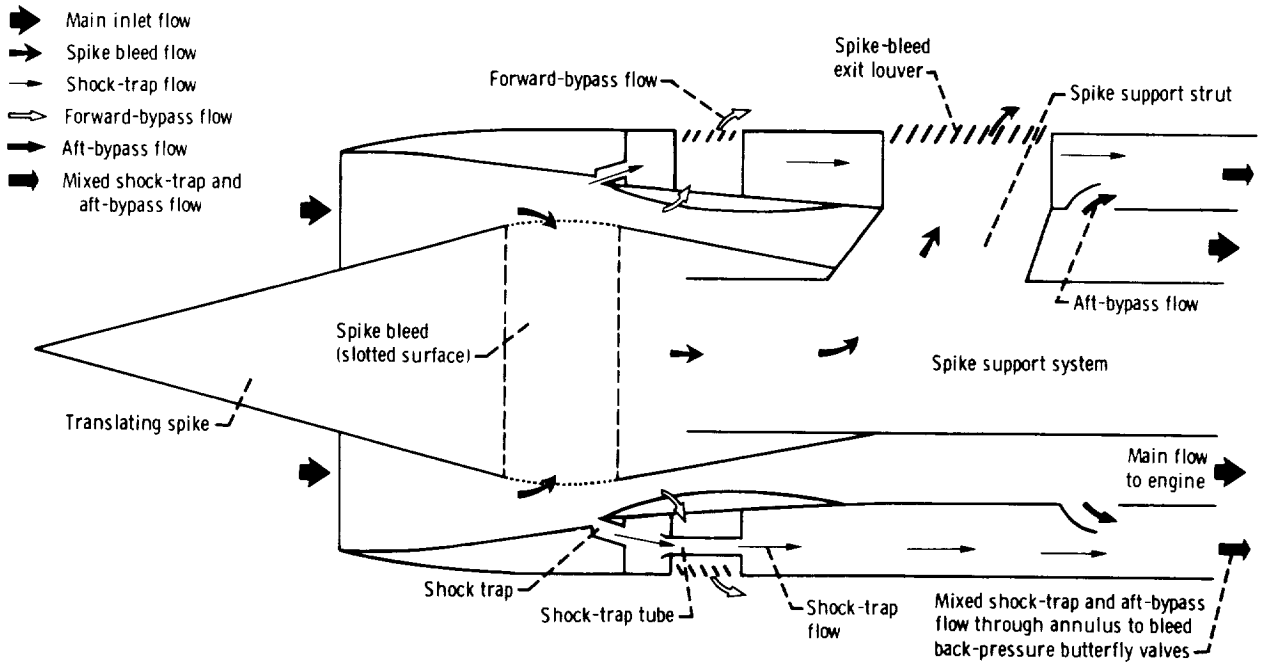

Figure 1. - Schematic diagram of inlet geometry and locations of bleeds and bypasses.

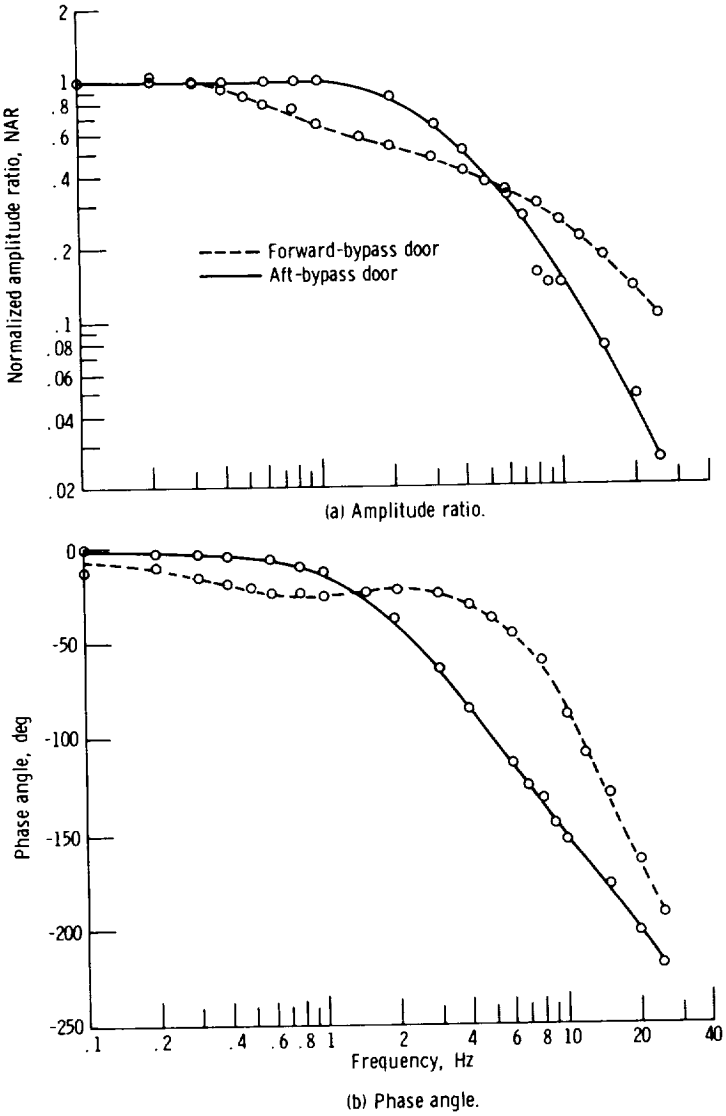

Figure 2. - Frequency response of forward- and aft-bypass position to command voltage. (Commanded peak-to-peak amplitude, 10 percent of maximum door area for forward-bypass and 20 percent for aft-bypass.)

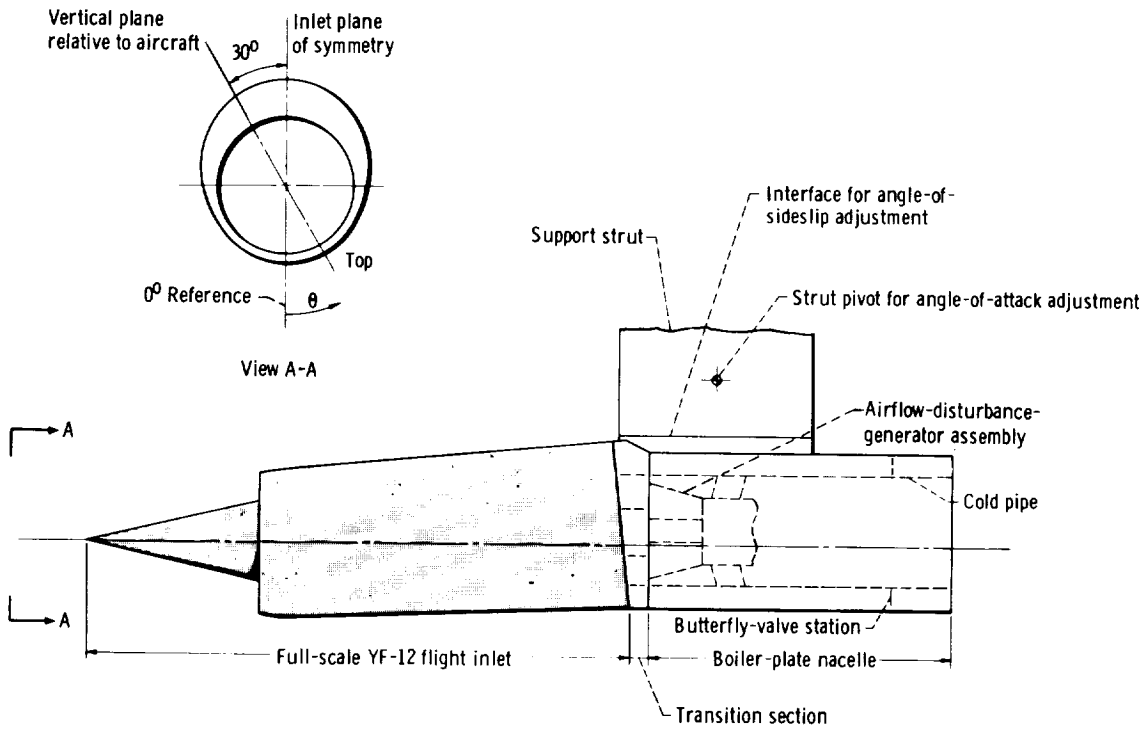

Figure 3. - Schematic diagram of inlet installation in test section of 10- by 10-Foot Supersonic Wind Tunnel.

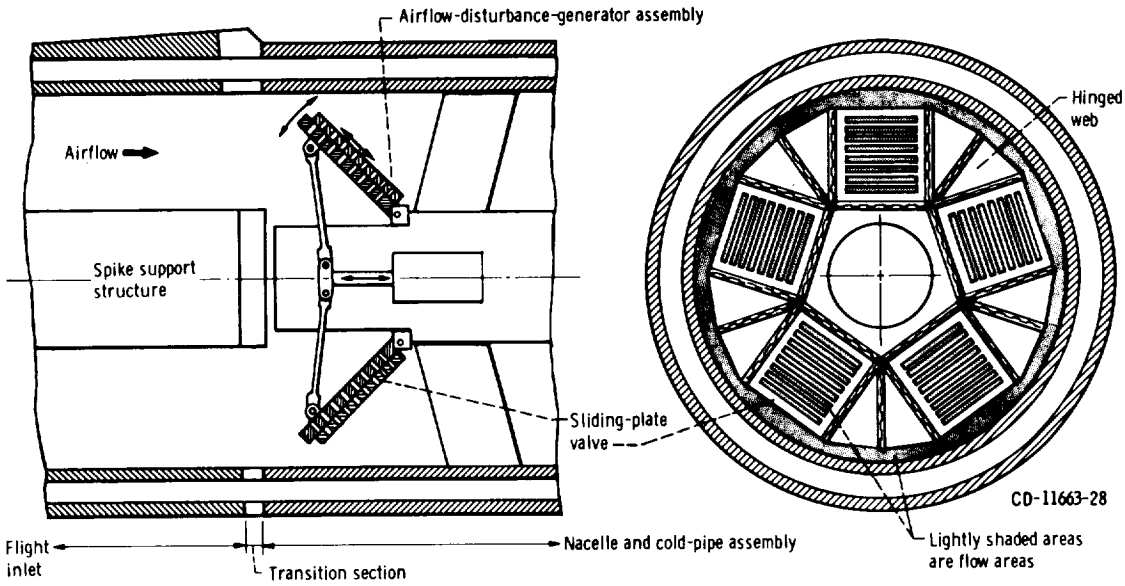

Figure 4. - Schematic diagram of airflow-disturbance generator.

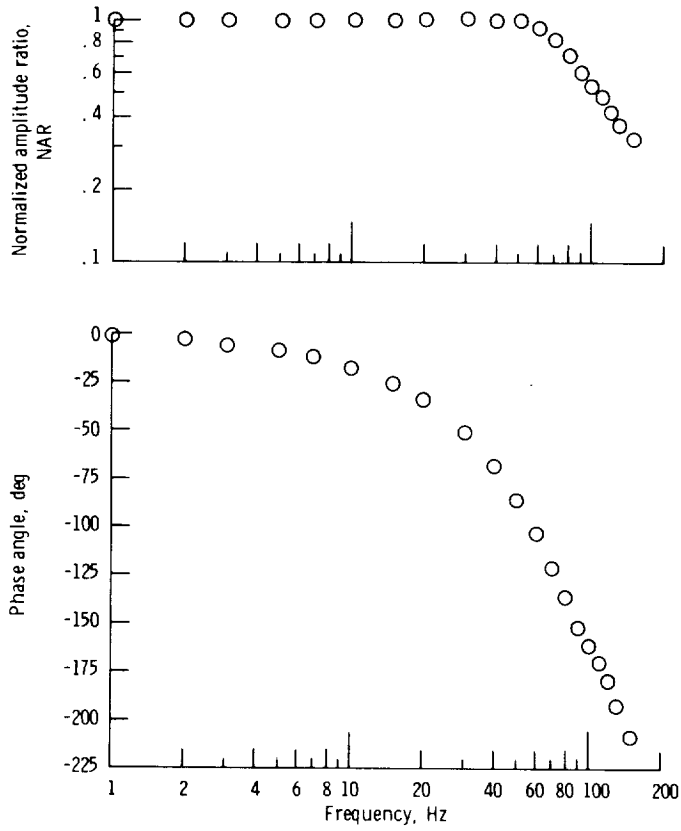

Figure 5. - Frequency response of airflow-disturbance-generator sliding-plate valve (disturbance door) position to position command voltage. (Commanded peak-to-peak amplitude, 10 percent of maximum valve area.)

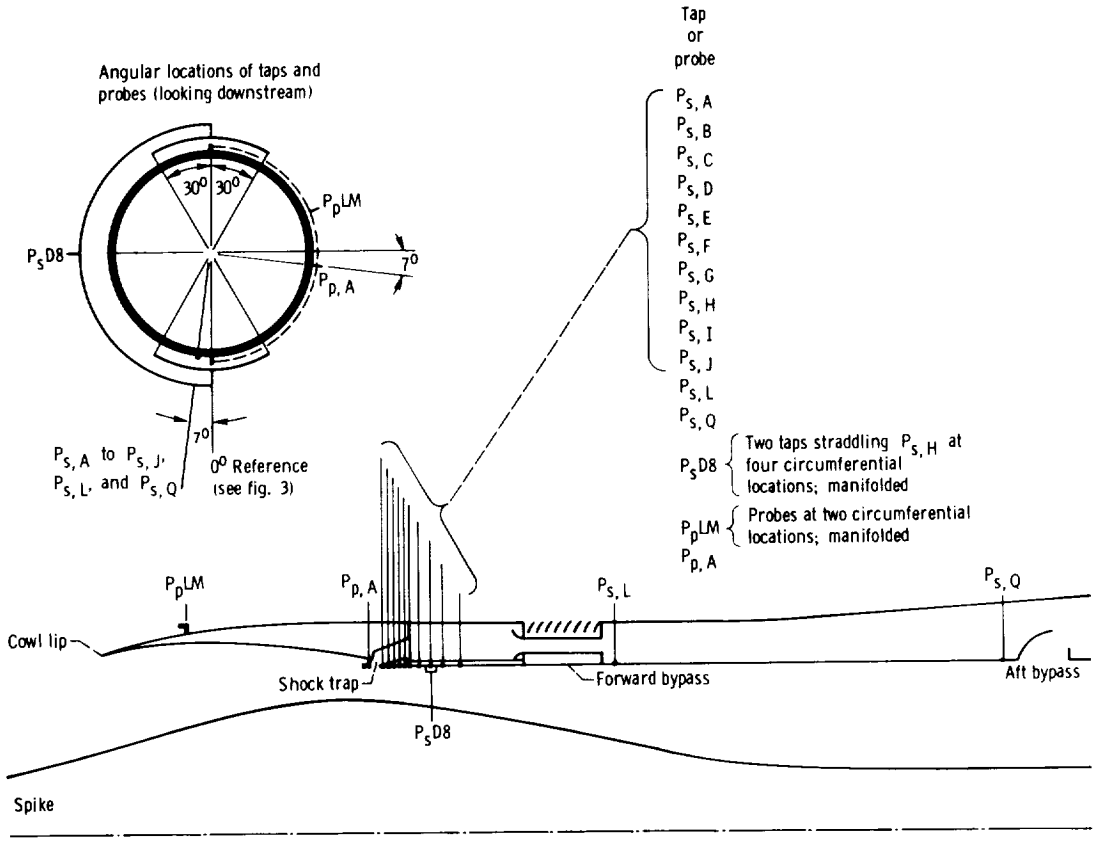

Figure 6. - Schematic diagram showing locations of static- and total-pressure measuring stations connected to high-response transducers.

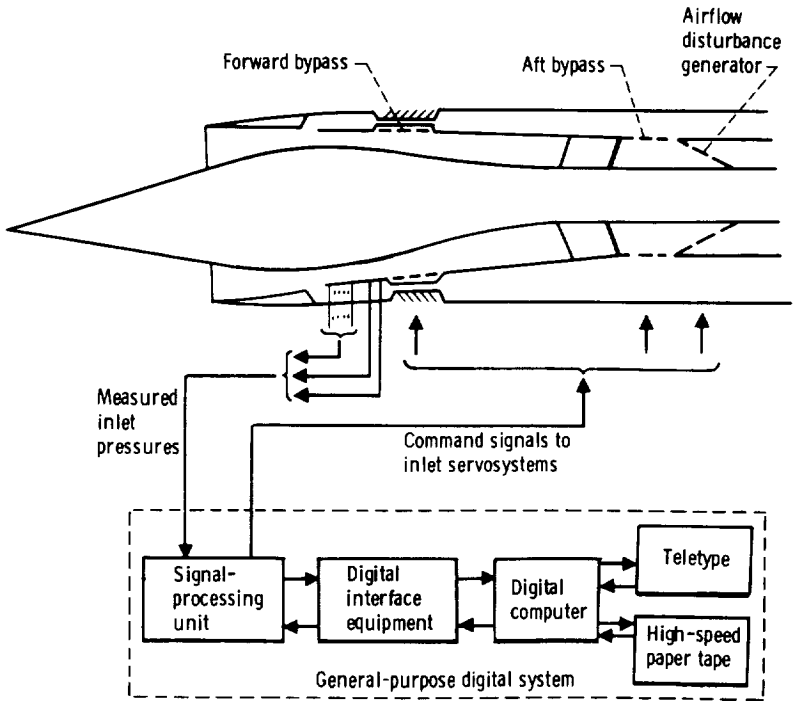

Figure 7. - Schematic representation of experimental setup in the 10- by 10-Foot Supersonic Wind Tunnel.

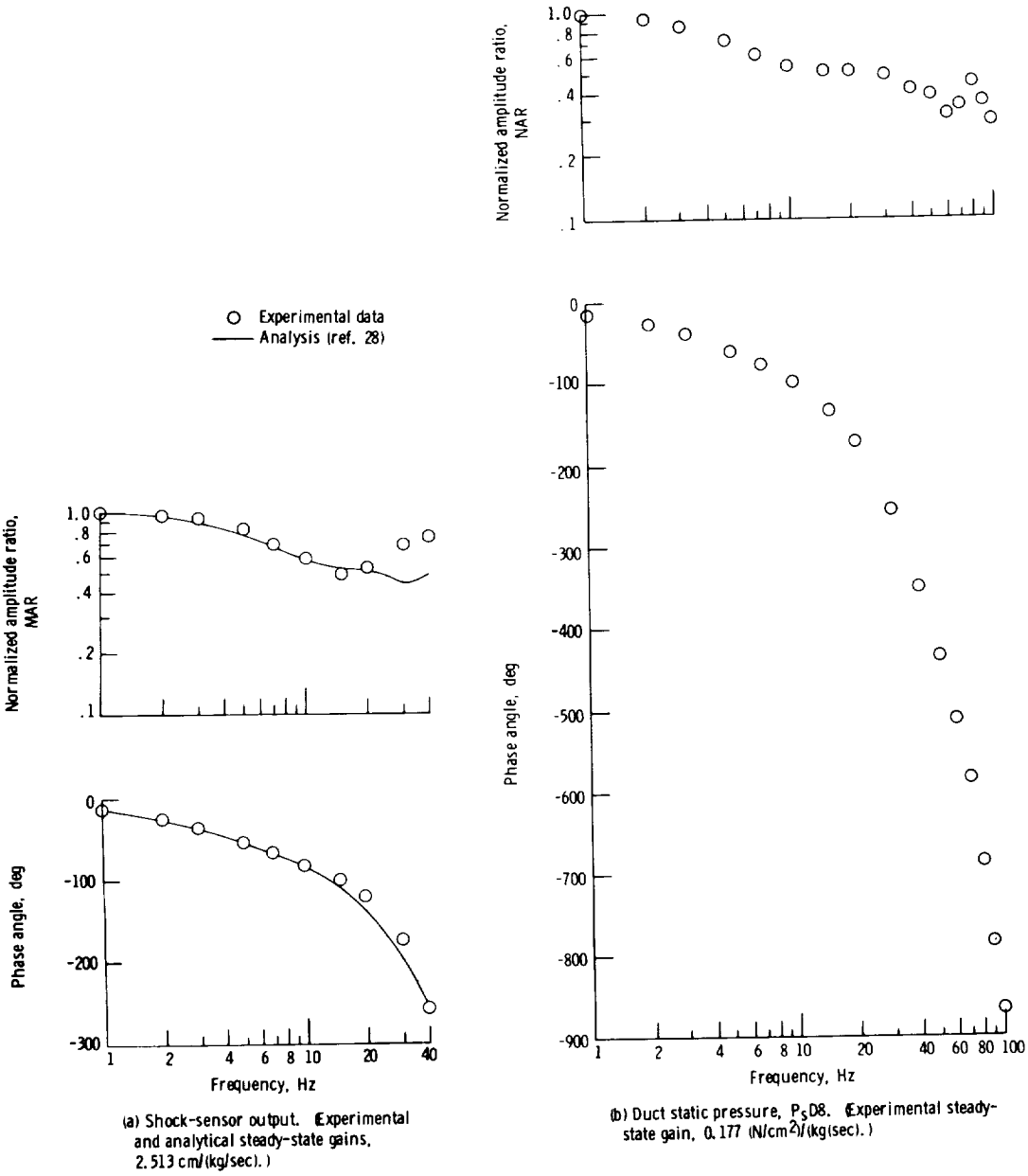

(a) Shock-sensor output. (Experimental and analytical steady-state gains, 2.513 cm/(kg/sec).)

(b) Duct static pressure, $P_{S}D8$. (Experimental steady-state gain, 0.177 $(N/cm^2)/(kg(sec).)$

Figure 8. - Inlet signal responses to airflow-disturbance generator at Mach 2.956 conditions.

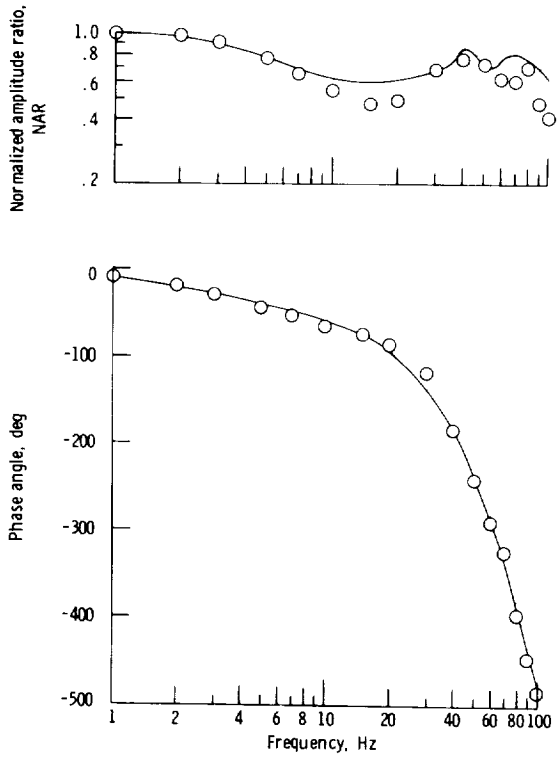

(c) Throat-exit static pressure, $P_{s,I}$. (Experimental steady-state gain, 0.104 $(N/cm^2)/(kg/sec)$; analytical steady-state gain, 0.066 $(N/cm^2)/(kg/sec)$.)

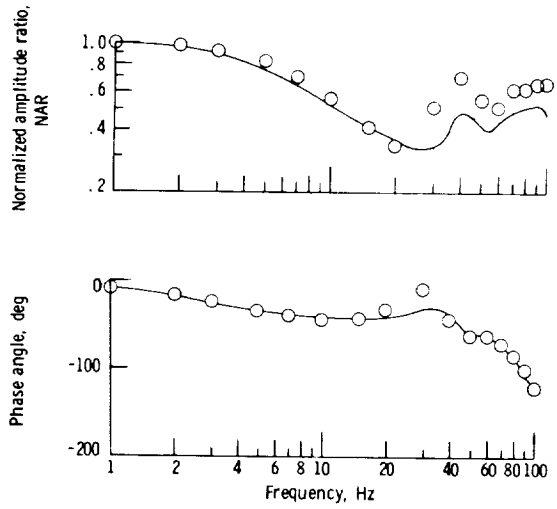

(d) Diffuser-exit static pressure, $P_{s,Q}$. (Experimental steady-state gain, 0.060 $(N/cm^2)/(kg/sec)$; analytical steady-state gain, 0.044 $(N/cm^2)/(kg/sec)$.)

Figure 8. - Concluded.

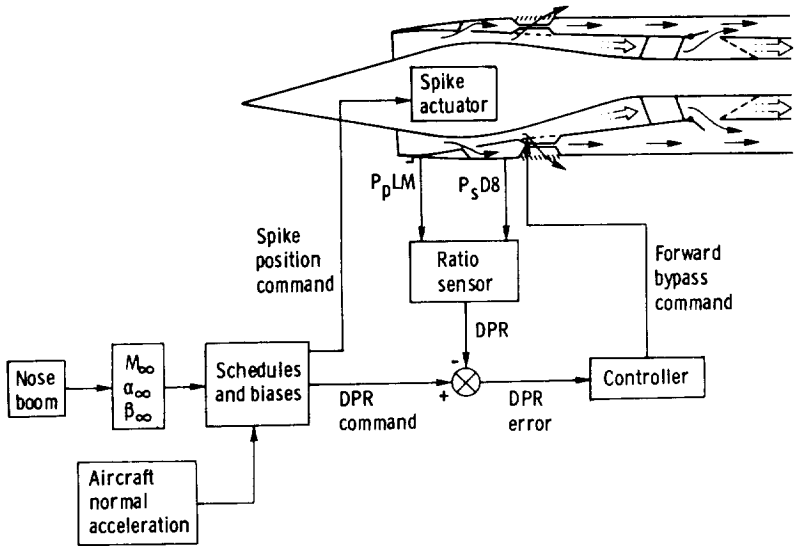

Figure 9. - Schematic of YF-12 aircraft inlet control system.

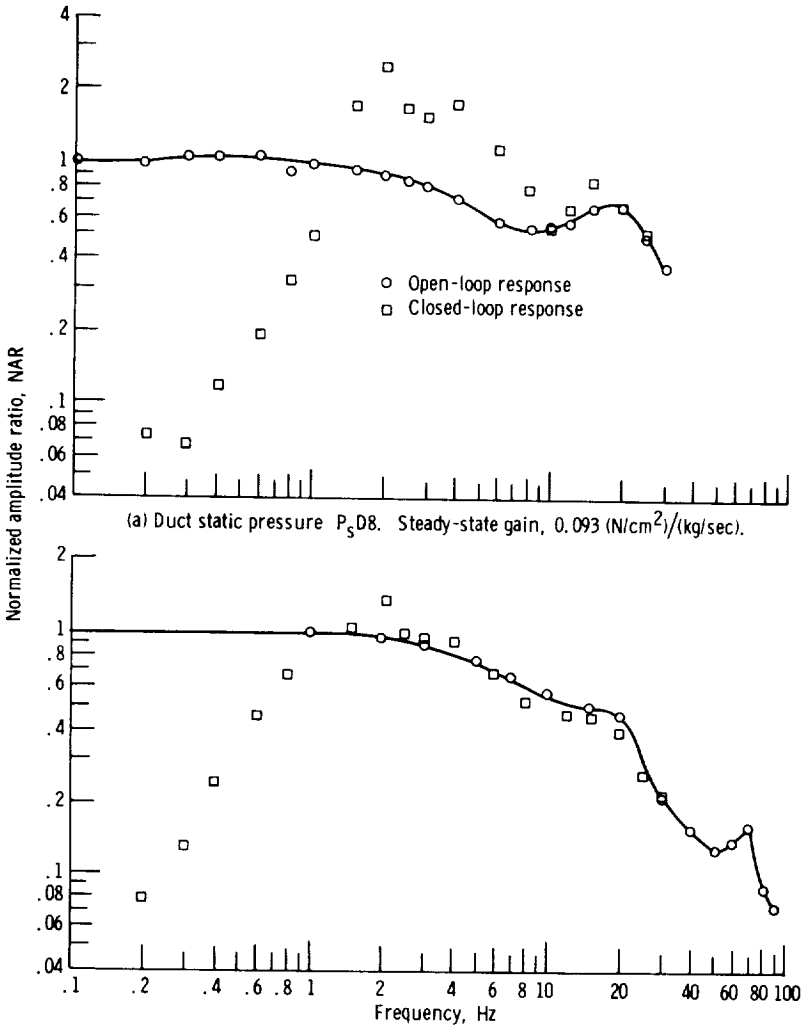

Figure 10. - Frequency responses of two inlet signals to airflow-disturbance generator, at Mach 2.474 conditions, with and without the duct-pressure-ratio control system of the aircraft.

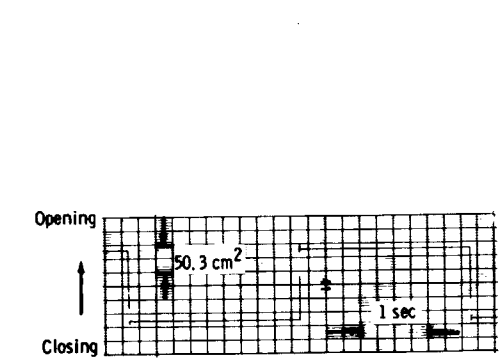

(a) Open-loop responses.

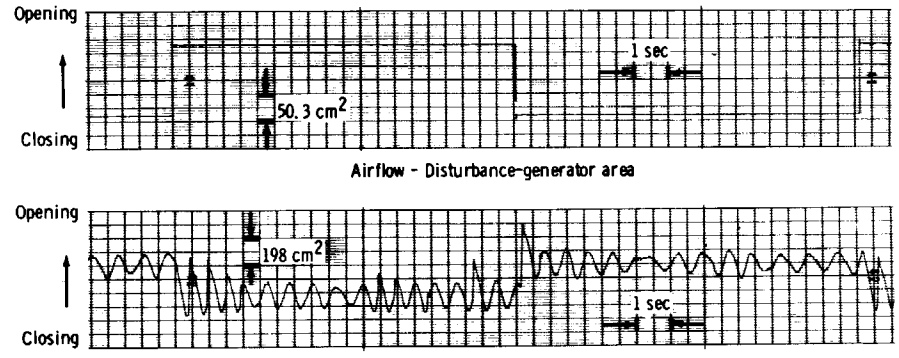

(b) Closed-loop responses.

Figure 11. - Transient response of the duct-pressure-ratio control system of the YF-12 aircraft to the airflow-disturbance generator at Mach 2.474 conditions.

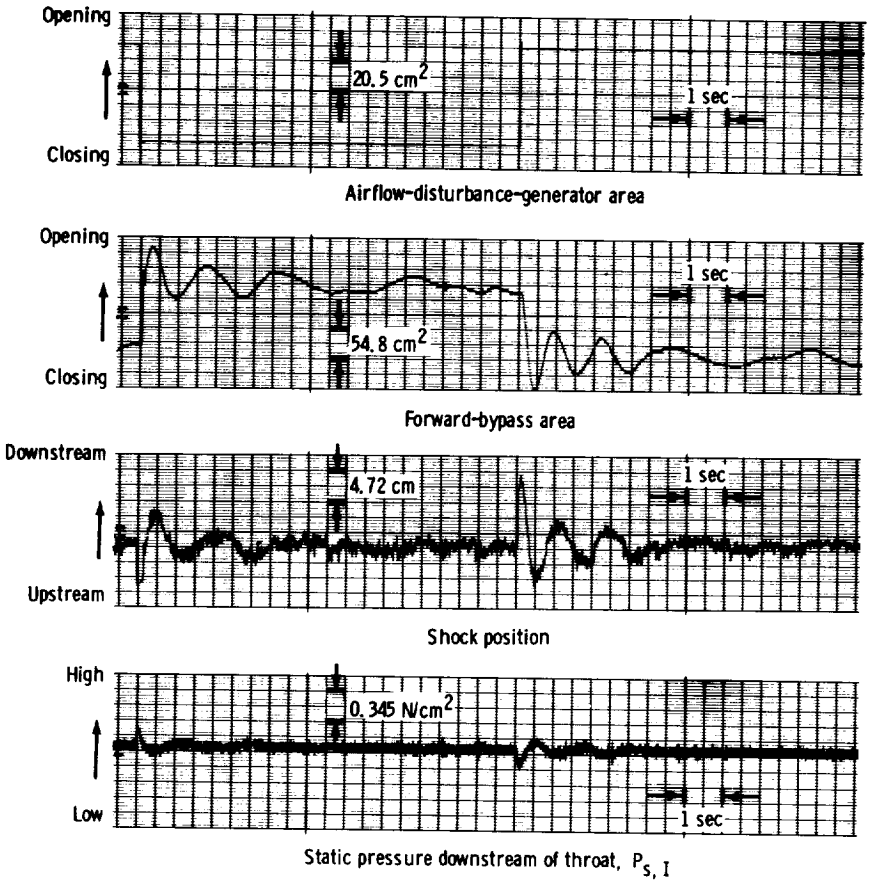

Figure 12. - Closed-loop transient responses of the YF-12 aircraft duct-pressure-ratio control system at reduced gain to the airflow-disturbance generator at Mach 2.474 conditions.

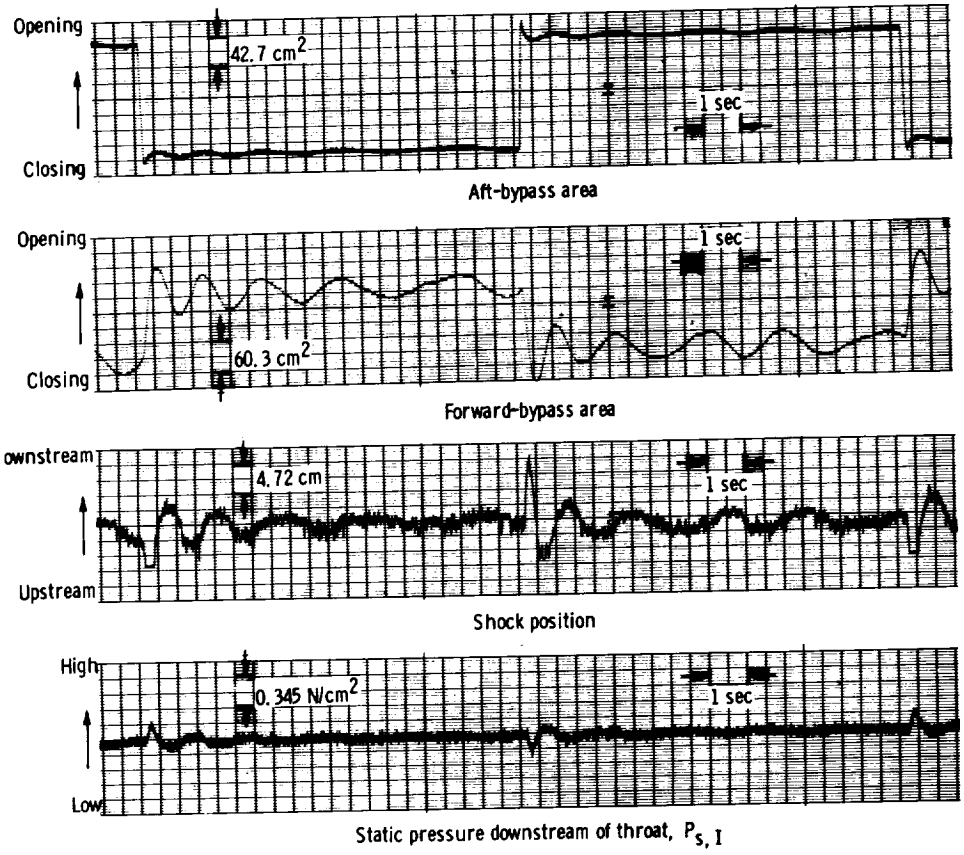

Figure 13. - Closed-loop transient responses of the YF-12 aircraft duct-pressure-ratio control system at reduced gain to an aft-bypass disturbance at Mach 2.474 conditions.

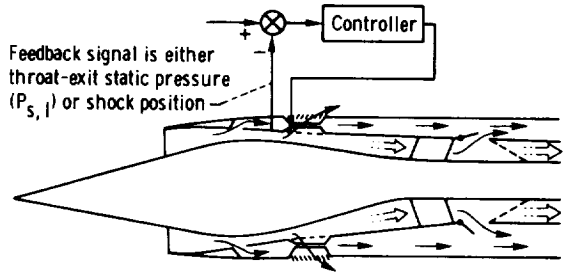

(a) Type-I control.

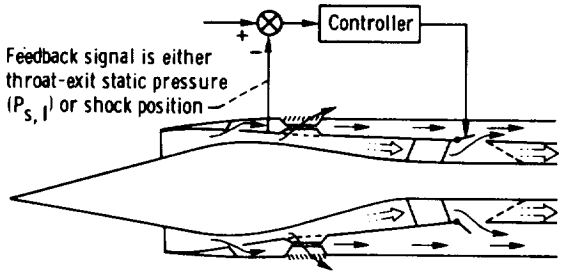

(b) Type-II control.

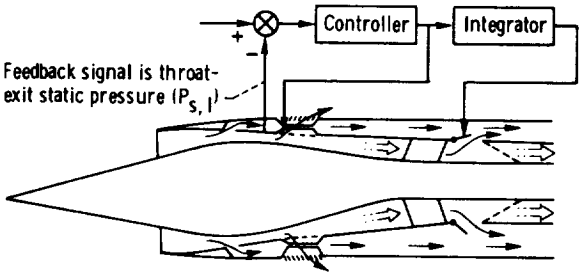

(c) Type-III control.

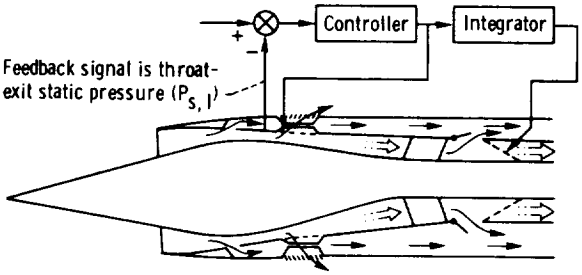

(d) Type-IV control.

Figure 14. - Block diagrams of experimental, proportional-plus-integral, shock-position controls for YF-12 aircraft inlet.

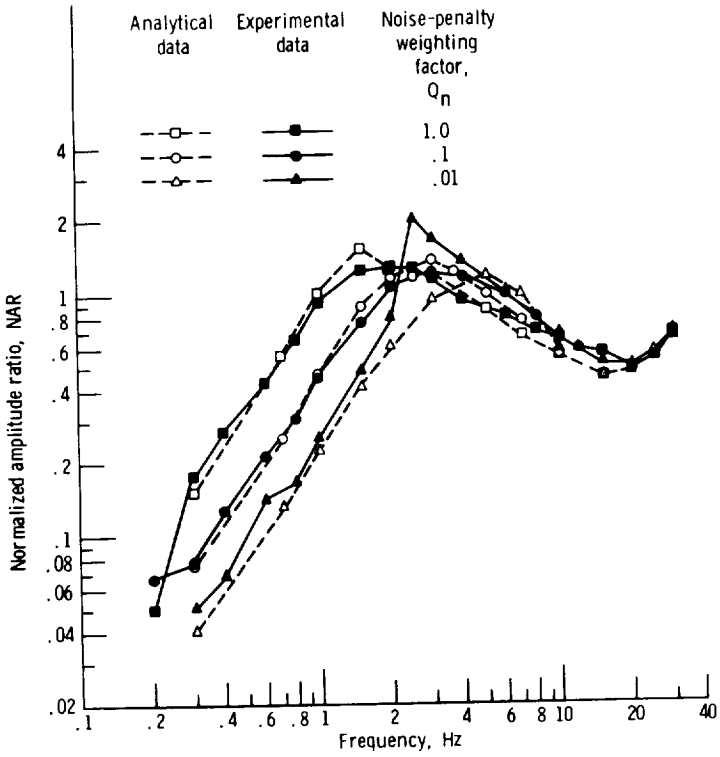

Figure 15. - Analytical and experimental closed-loop frequency responses of throat-exit static pressure $P_{s,I}$ for type-I controller with $P_{s,I}$ as feedback signal for various values of noise-penalty weighting factor Q_n. Mach 2.956 conditions.

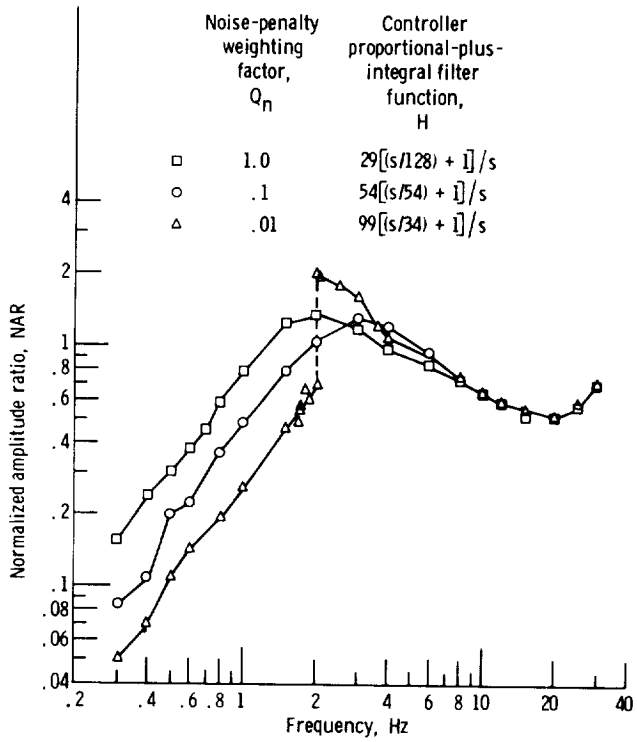

Figure 16. - Experimental closed-loop frequency responses of throat-exit static pressure $P_{s,I}$ for various values of noise-penalty weighting factor Q_n showing effect of non-linearity. Type-I control system. Mach 2.956 conditions.

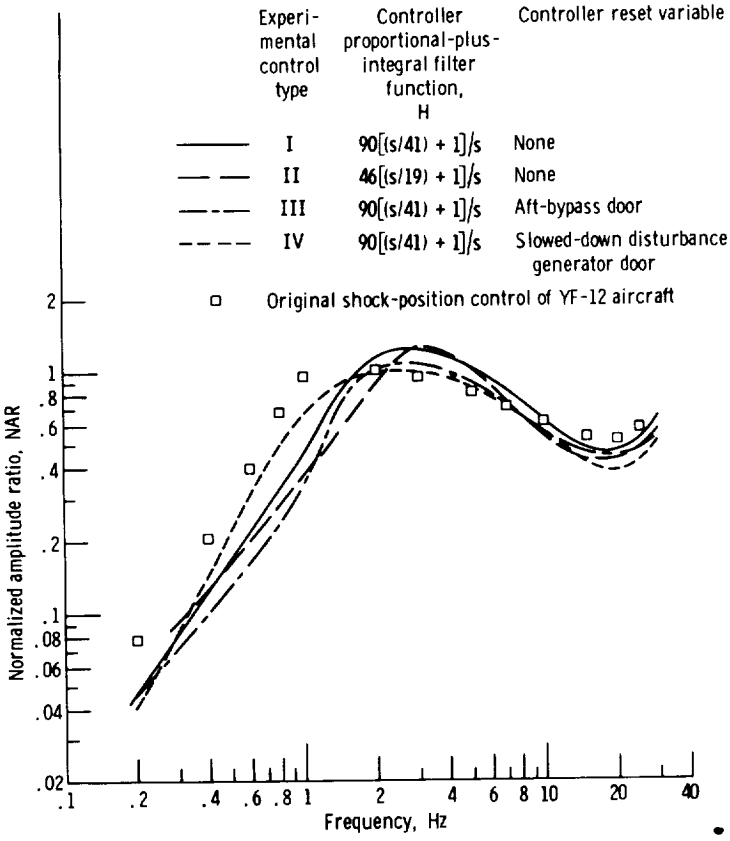

Figure 17. - Comparison of shock-position frequency responses of experimental controls with response of original shock control of YF-12 aircraft. Throat-exit static pressure $P_{s,I}$ used as feedback signal for experimental controls, and duct static pressure $P_{s}D8$ used as feedback for shock control of aircraft. Noise-penalty weighting factor Q_n for experimental controls was 0.1. Airflow-disturbance generator used as disturbance. Mach 2.956 conditions.

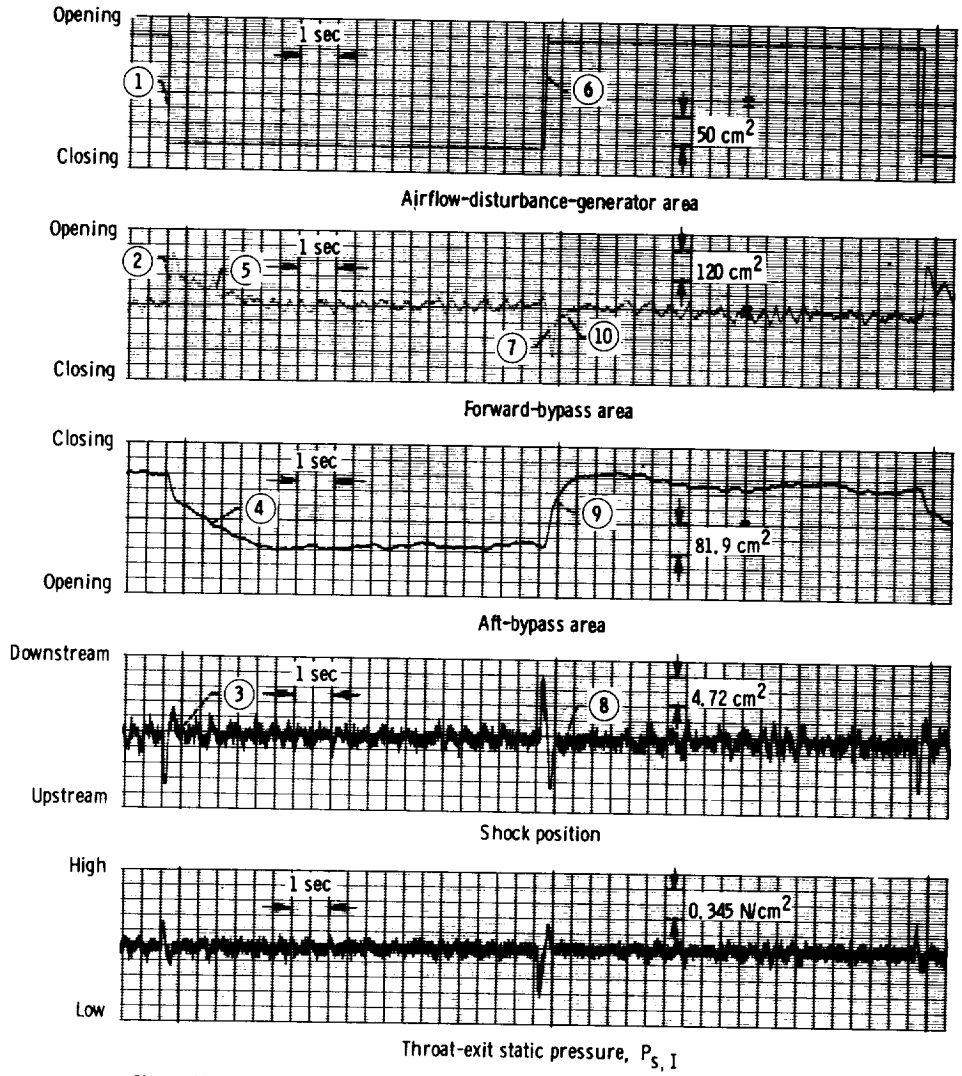

Figure 18. - Transient responses of type-III experimental shock-position control. Controller proportional-plus-integral filter function H was 90.4[(s/40.8) + 1]/s. Mach 2.956 conditions.